Low-Coordinate Barium Boryloxides: Synthesis and Dehydrocoupling Catalysis for the Production of Borasiloxanes

Erwann Le Coz, Vincent Dorcet, Thierry Roisnel, Sven Tobisch, J-F Carpentier, Yann Sarazin

Low-Coordinate Barium Boryloxides: Synthesis and Dehydrocoupling Catalysis for the Production of Borasiloxanes

Erwann Le Coz,[a] Vincent Dorcet,[a] Thierry Roisnel,[a] Sven Tobisch,*[b] Jean-François Carpentier,[a] and Yann Sarazin*[a]

Abstract: The first soluble barium boryloxides [Ba]–OB{CH(SiMe$_3$)$_2$} are presented. These mono- or dinuclear complexes feature low coordination numbers, as low as two for [Ba(OB{CH(SiMe$_3$)$_2$}$_2$)$_2$], which is further stabilized by intra- and intermolecular Ba···H$_3$C agostic interactions. Ba–boryloxides and the parent [Ba{N(SiMe$_3$)$_2$}$_2$.(thf)$_2$] catalyze the dehydrocoupling of borinic acids with hydrosilanes, providing borasiloxanes under mild conditions.

Complexes of the large alkaline earths (= Ae) calcium, strontium and barium are increasingly used in molecular catalysis as alternatives to mainstream late transition metal catalysts.[1] These developments can be paralleled with the many breakthroughs in the organometallic chemistry of calcium,[2-4] while in comparison progress with strontium[5] and barium [6] has been slow owing to greater synthetic challenges. Ca^{2+} (r_{ionic} = 1.00 Å), Sr^{2+} (1.18 Å) and Ba^{2+} (1.35 Å) are large, electropositive ions that generate highly ionic d^0 complexes. Despite their trademark reactivity that generally increases upon descending group 2, heteroleptic Ae complexes may be plagued by ligand scrambling. Hence, although they often demonstrate the best aptitude in catalysis,[1,7] barium complexes can also suffer from excessive basicity, kinetic lability, and propensity to form polynuclear, insoluble species.[8]

Discrete molecular barium alkoxides are scarce. Barium is characterized by its large size, affinity for high (8 or more) coordination numbers, and pronounced oxophilicity and electropositivity. With regular alcohols, e.g. ^{t}BuOH, it yields polymeric alkoxides of low solubility that sometimes decompose to oxoclusters.[9] The first authenticated soluble Ba–alkoxide was the 8-coordinate [Ba{κ^4-N(CH$_2$CH$_2$O)(CH$_2$CH$_2$OH)$_2$}$_2$].[10] The dinuclear [Ba$_2$(μ^2-OCPh$_3$)$_3$(OCPh$_3$)(thf)$_3$] was obtained from bulky Ph$_3$SiOH,[11] while diethylene glycol returned [Ba{κ^3-O(CH$_2$CH$_2$O)$_2$}{κ^3-O(CH$_2$CH$_2$OH)$_2$}$_2$].[12] The presence of CF_3 groups in α position to the alkoxide stabilizes Ba–fluoroalkoxides.[13] Siloxides are derivatives of alkoxides that produce mono-[14] and dinuclear Ba species[12,15] or even higher aggregates,[16] the seminal example being Caulton's [Ba$_2$(μ^2-OSi^{t}Bu$_3$)$_3$(OSi^{t}Bu$_3$)(thf)].[12] Yet, nothing is known about Ba–boryloxides, in spite of occurrences for other main group metals,[17] including magnesium.[18] Due to delocalization of the *O* atom lone pairs in the empty p_z orbital at boron, boryloxides R$_2$BO$^-$ may be seen as electron poor analogues of alkoxides, or even of ketones or ketyl radicals. On this account, and in conjunction with its great steric demands, we reasoned that {(Me$_3$Si)$_2$CH}$_2$BO$^-$ should afford soluble, low coordinate, highly electrophilic and hence reactive barium species. This strategy met with success, and we report herein on the first Ba–boryloxides, that exhibit low coordination numbers (2-4): [Ba{OB(CH(SiMe$_3$)$_2$)$_2$}$_2$], Ba{OB(CH(SiMe$_3$)$_2$)$_2$}$_2$.(thf)$_2$], and [Ba{μ^2-N(SiMe$_3$)$_2$}{OB(CH(SiMe$_3$)$_2$)$_2$}]$_2$.

In addition, we reveal how these complexes, as well as their [Ba{N(SiMe$_3$)$_2$}$_2$.(thf)$_2$] congener, catalyze the dehydrocoupling of borinic acids and hydrosilanes to yield borasiloxanes. These molecules containing [B–O–Si] motifs are precursors to borosilicate materials,[19] heat and chemical resistant polymers, and polymer sensors.[20] Classical routes to borasiloxanes imply the condensation of various boron- and silicon-based reagents, but they are not atom-efficient and often entail drawbacks such as release of toxic/corrosive wastes and lack of selectivity.[21] Instead, a few catalyzed processes pairing silanols or hydrosilanes with hydroboranes, diboranes, boraxanes or vinylboronates were disclosed recently; they rely on late transition metal complexes[22] or Mo(CO)$_6$.[23] None involves a main group metal catalyst, a dehydrocoupling procedure, or the utilization of borinic acids. Such methodology is unveiled here, and preliminary kinetic and mechanistic insights are also provided.

The thf solvate [Ba(OB{CH(SiMe$_3$)$_2$}$_2$)$_2$.(thf)$_2$] (**2**.(thf)$_2$; See the Supporting Information for its XRD structure) was obtained in near quantitative yield upon reaction of the borinic acid {(Me$_3$Si)$_2$CH}$_2$BOH (R$_2$BOH) with [Ba{N(SiMe$_3$)$_2$}$_2$.(thf)$_2$] (**1**, Scheme 1). This mononuclear complex, the first barium boryloxide, cannot be isolated free of thf by this protocol. The heteroleptic dimer [Ba{μ^2-N(SiMe$_3$)$_2$}(OB{CH(SiMe$_3$)$_2$}$_2$)]$_2$ (**3**) was prepared in 85% yield by equimolar reaction of **1** and R$_2$BOH. Treatment of **3** with 2 equiv of R$_2$BOH in petroleum ether afforded [Ba(OB{CH(SiMe$_3$)$_2$}$_2$)$_2$] (**2**), a unique two-coordinate barium complex (Scheme 1). Considering the oxophilicity and natural π-donating ability of oxygen atoms in the chemistry of oxophilic metals, the relative ease of synthesis, stability and good solubility of **2** are remarkable. All three complexes are air-sensitive colorless solids, with excellent solubility in common organic solvents, including aliphatic hydrocarbons.

The solid-state structure of the centro-symmetric dimer **3** presents remarkable features, notably a rare[24] three-coordinate environment about the metals with a rhomboidal Ba$_2$N$_2$ central core and boryloxides in terminal positions (Figure 1).

[a] E. Le Coz, Dr. V. Dorcet, Dr. T. Roisnel, Prof. Dr. J-F. Carpentier, Dr. Y. Sarazin
Univ Rennes, CNRS, ISCR (Institut des Sciences Chimiques de Rennes) – UMR 6226, F-35000 Rennes (France)
E-mail: yann.sarazin@univ-rennes1.fr
[b] Dr. S. Tobisch
School of Chemistry
University of St Andrews
Purdie Building, North Haugh, St Andrews KY16 9ST (UK)
E-mail: st40@st-andrews.ac.uk

Supporting information for this article is given via a link at the end of the document.

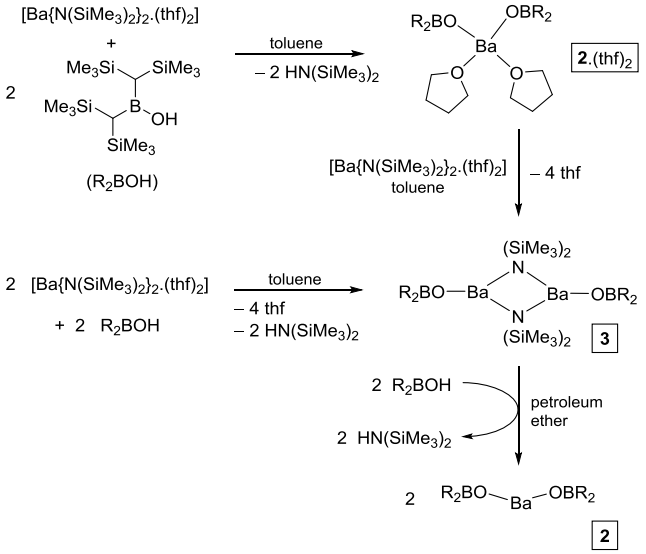

Scheme 1. Syntheses of low-coordinate [Ba]-boryloxides.

In related cases of supported heteroleptic amido/alkoxo barium dimers, the dinuclear edifices are bridged through the $O_{alkoxide}$ atoms.[15,25] The bonding situation in **3** reflects both considerable steric bulk of the boryloxide R_2BO^- and limited electronic density available at $O_{boryloxide}$ to bridge the two metals. The geometry about Ba1 is distorted trigonal planar (Σ_θ(Ba1) = 348.2°). The N1–Ba1–N1^i angle of 82.34(5)° in **3** correlates to that in [Ba{μ^2-N(SiMe$_3$)$_2$}{N(SiMe$_3$)$_2$}]$_2$ (81.89(11)°).[24a] The Ba–N_{bridge} distances in this complex are commensurate (2.799(4) and 2.846(4) Å), but they deviate much in **3** (2.721(2) and 2.891(2) Å).

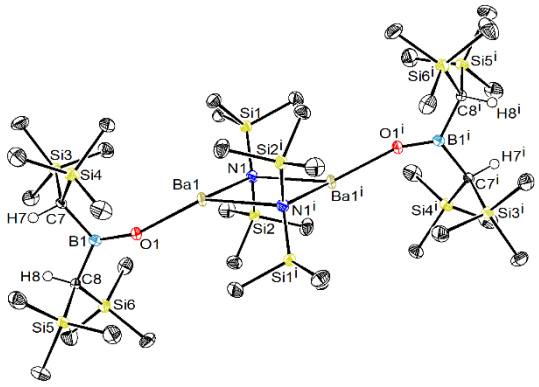

Figure 1. ORTEP representation of [Ba{μ^2-N(SiMe$_3$)$_2$}(OB{CH(SiMe$_3$)$_2$}$_2$)]$_2$ (**3**). Ellipsoids at the 50% probability level. H atoms (other than BC*H*) omitted for clarity. Selected bond lengths (Å) and angles (°): Ba1–O1 = 2.3999(14), Ba1–N1 = 2.7210(16), Ba1–N1^i = 2.8912(17), O1–B1 = 1.332(3); O1–Ba1–N1 = 121.64(5), O1–Ba1–N1^i = 144.18(5), N1–Ba1–N1^i = 82.34(5), B1–O1–Ba1 = 160.00(14), O1–B1–C8 = 123.38(18), O1–B1–C7 = 120.05(18), C8–B1–C7 = 116.57(17).

The molecular structure of **2** (Figures 2 and 3) depicts an unprecedented two-coordinate barium complex. The Ba–O interatomic distances in **2** (2.384(2) and 2.410(2) Å) match that in **3** (2.400(2) Å). The O1–Ba1–O21 angle of 130.59(6)° is far from the ideal linear geometry. This likely results from multiple Ba···H$_3$C intramolecular (4) and intermolecular (4) agostic interactions with methyl groups from neighboring SiMe$_3$ moieties (Figure 3). The corresponding eight Ba1–H distances range within 2.799(3)–3.119(3) Å;[26] the Ba–C distances to the carbon atoms bearing the relevant hydrogens are in the range 3.258(3)-3.886(3) Å. The relatively narrow angles B2–O1–Ba1 (162.85(16)°) and B22–O21–Ba1 (156.46(15)°) testify to a limited contribution of the lone pairs on the O atoms to the Ba–O and B–O bonds.

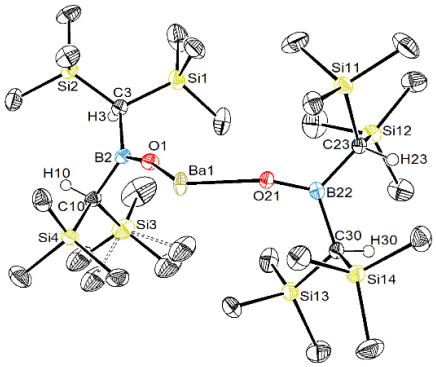

Figure 2. ORTEP representation of [Ba(OB{CH(SiMe$_3$)$_2$}$_2$)$_2$] (**2**). Ellipsoids at the 50% probability level. Minor components in disordered Me groups shown in dotted bonds. H atoms (other than BC*H*) and Ba···H$_3$C interactions omitted for clarity. Selected bond lengths (Å) and angles (°):Ba1–O1 = 2.3842(16), Ba1–O21 = 2.4098(16), O1–B2 = 1.333(3), O21–B22 = 1.331(3); O1–Ba1–O21 = 130.59(6), B2–O1–Ba1 = 162.85(16), B22–O21–Ba1 = 156.46(15), O1–B2–C3 = 120.70(2), O1–B2–C10 = 120.10(2), C3–B2–C10 = 119.20(2), O21–B22–C23 = 121.00(2), O21–B22–C30 = 120.30(2), C23–B22–C30 = 118.71(19).

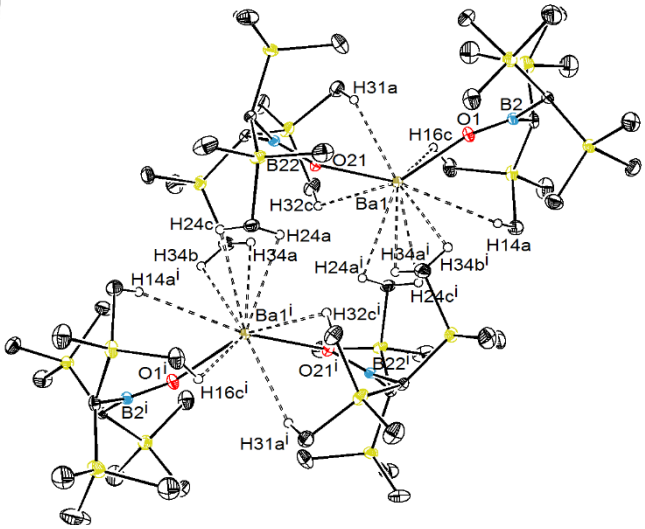

Figure 3. Representation of the molecular structure of [Ba(OB{CH(SiMe$_3$)$_2$}$_2$)$_2$] (**2**), showing the pattern of eight Ba···H$_3$C intra- and intermolecular interactions in dotted lines. H atoms other than those interacting with Ba are omitted for clarity. Only the main component of the disordered SiMe$_3$ fragment is depicted. Pertaining Ba–H interatomic distances (Å): Ba1–H14A = 3.119(3), Ba1–H16C

= 2.932(3), Ba1–H31A = 2.799(3), Ba1–H32C = 2.998(3), Ba1–H24A' = 2.969(3), Ba1–H24C' = 3.044(3), Ba1–H34A' = 2.931(3), Ba1–H34B' = 2.957(3).

State-of-the-art DFT computations[27] have been employed to further characterise the bonding pattern in **2** and **3**. Natural Population Analysis (NPA) and Bader's quantum theory of atoms in molecules (QTAIM) methodology have been applied. As far as the bonding situation in the rhomboidal Ba_2N_2 central unit in **3** is concerned, QTAIM succeeded in locating bonding paths connecting barium with N_{amide} and $O_{boryloxide}$ featuring bond critical points (BCPs) that are shifted towards the electropositive alkaline earth. The QTAIM topological parameter, *viz*. electron density ρ(r) and its second derivative, the Laplacian $\nabla^2\rho$(r), derived at the located BCPs are particularly informative. As detailed in Figure 4, ρ(r) values are rather small (~0.03 *e*Å^{-3}) with $\nabla^2\rho$(r) adopting a positive sign. All this is indicative of the predominant electrostatic nature of Ba–N and B–O bonds, which are also considerably polarised. The likelihood for forming a dimer featuring a Ba_2O_2 central unit has also been probed. The corresponding μ-OBR_2 bridged compound **3'** exhibits similar topological QTAIM parameter but is found 5.3 kcal mol^{-1} above **3**. In light of the primarily electrostatic bonding situation, the lower ability of **3'** to involve bridging across a more electron deficient $O_{boryloxide}$ becomes understandable, while steric crowding inflicted by the bulky boryloxide also plays a role.

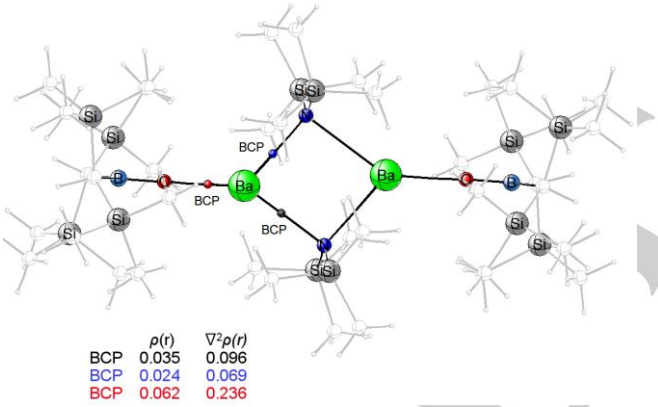

Figure 4. Topological QTAIM parameter (electron density ρ(r) in eÅ^{-3} and its Laplacian $\nabla^2\rho$(r) in eÅ^{-5}) of crucial bond critical points (BCP) located for [Ba{μ^2-N(SiMe$_3$)$_2$}(OB{CH(SiMe$_3$)$_2$}$_2$)]$_2$ (**3**).

The stabilising influence of Ba···H_3C interactions in **2** has been probed first by means of QTAIM. Unfortunately, a bonding path describing such interaction could not be found.[28] It prompted us to evaluate to what degree dispersive forces influence the energy gap between **2** with a bent O–Ba–O unit and hypothetical **2'** featuring a linear O–Ba–O alignment, which thus is less prone to Ba···H_3C interactions. Employing DFT with and without dispersion corrections revealed a widening of the gap by about two thirds due to an increased stability of **2** by dispersive interactions. It let us reasonably conclude that Ba···H_3C interactions are likely vital for the stability of **2**.

Complexes **2**, **2**.(thf)$_2$ and **3**, as well as the bis-amide **1**, catalyze the dehydrocoupling of R_2BOH and hydrosilanes. The coupling with $PhSiH_3$ in C_6D_6 at 60 °C produced the borasiloxane $PhSi(H)_2OBR_2$ (**P$_1$**) in high yields, and conversion was monitored by NMR spectroscopy. The thf-free dimer [Ba{N(SiMe$_3$)$_2$}$_2$]$_2$ also generates **P$_1$**, but it is much too fast to enable reliable kinetic monitoring; yet, although we excluded it from our kinetic investigations for practical reasons, this precatalyst constitutes per se the most synthetically effective precatalyst for BO–H/H–Si dehydrocouplings. For each of the four precatalysts, the semi-logarithmic plots of $PhSiH_3$ conversion vs. time is linear, indicating a first-order dependence in [$PhSiH_3$]. The respective apparent rate constants k_{app} were of the same magnitude (k_{app}: **1**, 2.19(5) h^{-1}; **2**, 0.64(1) h^{-1}; **2**.(thf)$_2$, 0.52(1) h^{-1}; **3**, 1.18(1) h^{-1}), establishing about equal proficiency for all precatalysts, and indicating that [Ba]–OBR_2 species are involved in the catalytic manifold. Upon addition of 1 or even 2 equiv of $HN(SiMe_3)_2$ vs. Ba, the reaction rates for **2**.(thf)$_2$ (0.45(1) and 0.57(1) h^{-1}) remained near identical to those of **2** and **2**.(thf)$_2$ alone, i.e. about 4-fold lower than that of **1**.[29] The easily accessed and most active **1** was selected for further kinetic studies. First order dependence in [$PhSiH_3$] was confirmed by the linear plot of ln(R_0) vs. ln([$PhSiH_3$]$_0$), where R_0 is the initial rate, for a range of initial concentrations [$PhSiH_3$]$_0$. The reaction rate is zeroth order in [R_2BOH]. It shows an unusual second order dependence in precatalyst concentration,[30] as evidenced by the linear variations of ln(k_{app}) vs. ln([**1**]) (slope = 2) and of k_{app} vs. [**1**]^2, and further corroborated by Burés' graphical method.[31] The kinetic rate law for the coupling of R_2BOH and $PhSiH_3$ mediated by **1** is hence expressed by:

$$R = -d[PhSiH_3]/dt = k.[\mathbf{1}]^2.[PhSiH_3] \quad (1)$$

where k is the rate constant. These data are consistent with a catalytic cycle that evolves through a dinuclear transition state. Eyring analysis (T^{re} = 20–70 °C) shows the reaction is kinetically facile, with $\Delta H^{\ddagger}$ = 9.1(2) kcal mol^{-1}, $\Delta S^{\ddagger}$ = –24.2(8) cal mol^{-1} K^{-1} indicative of a highly ordered transition state, and $\Delta G^{\ddagger}$ = 16.4(5) kcal mol^{-1} at 25 °C. Under otherwise identical conditions, reaction rates decrease upon ascending group 2 for the congeneric precatalysts **1** , [Sr{N(SiMe$_3$)$_2$}$_2$.(thf)$_2$] and [Ca{N(SiMe$_3$)$_2$}$_2$.(thf)$_2$] (k_{app} = 2.19(5) h^{-1}, 1.80(1) h^{-1} and 0.082(1) h^{-1}, respectively), although the drop is more appreciable for Ca than for Sr.

Substrate scope was probed by tuning the nature of the hydrosilane coupled to R_2BOH in reactions catalyzed by **1** (Table 1). In the benchmark coupling of $PhSiH_3$ and R_2BOH, product **P1** was produced in 100% and 75% yields in 10 h using respectively 2 and 1 mol-% of precatalyst (entries 1 and 2). The production of **P$_1$** is chemoselective, as the formation of $PhSi(H)(OBR_2)_2$ was never detected. Catalysis does not proceed with Ph_2SiH_2 (entry 6). This is due to the identity of the substrate rather than catalyst decomposition, since quantitative formation of **P$_1$** was observed in a separate experiment where $PhSiH_3$ was added to the NMR tube 12 h after the initial addition of Ph_2SiH_2. Similarly, coupling does not occur between Ph_3SiH and R_2BOH. Commercially available alkoxyhydrosilanes (entry 7) and alkylhydrosilanes (entry 8) can be converted effectively, albeit the reactions are slower with these substrates. Compared to

$PhSiH_3$ (entry 2, k_{app} = 1.05(1) h^{-1}), reaction rates increase upon introduction of electron-withdrawing group in *para* position of the aromatic group (entries 3 and 4; k_{app} = 1.67(2) h^{-1}), whereas electron-donating groups inhibit the reaction (entry 5; k_{app} = 0.72(1) h^{-1}); these observations agree with the accumulation of a partial negative charge localized at silicon in the turnover-limiting step.

Table 1. Ba-catalysed dehydrocoupling of R_2BOH and $SiHR^1R^2R^3$ [a]

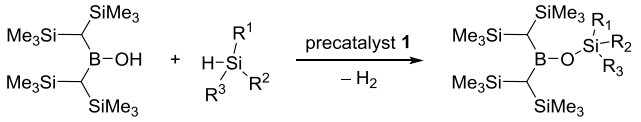

	Silane	[OH]/[SiH]/[**1**][b]	Product	Conv [%][c]
1	$PhSiH_3$	50:50:1	R_2BO-SiH_2Ph	100
2	$PhSiH_3$	100:100:1	R_2BO-SiH_2Ph	75
3	*p*-F-C_6H_4-SiH_3	50:50:1	R_2BO-SiH_2(*p*-F-C_6H_4)	100
4	*p*-F-C_6H_4-SiH_3	100:100:1	R_2BO-SiH_2(*p*-F-C_6H_4)	86
5	*p*-MeO-C_6H_4-SiH_3	100:100:1	R_2BO-SiH_2(*p*-MeO-C_6H_4)	63
6	Ph_2SiH_2[d]	10:10:1	R_2BO-$SiHPh_2$	0
7	$(^iPrO)_3SiH$[d]	10:10:1	R_2OB-$Si(O^iPr)_3$	62
8	^{n}BuSiH_3[e]	10:10:1	R_2OB-$SiH_2{}^n$Bu	89

[a] Reactions at 60 °C in C_6D_6 (0.6 mL), with [**1**]$_0$ = 1.69–16.9 mM; reaction times (10 h unless otherwise specified) not optimized. [b] Initial ratio $[R_2BOH]_0/[SiHR^1R^2R^3]_0/[\mathbf{1}]_0$. [c] Conversion of $HSiR^1R^2R^3$ evaluated by ^{1}H NMR spectroscopy, using C_6Me_6 as internal calibrant. [d] Reaction time = 12 h. [e] Reaction time = 48 h; conversion reached 70% after 24 h.

In conclusion, $\{(Me_3Si)_2CH\}_2BO^-$ enables the syntheses of discrete barium-boryloxide complexes featuring the lowest coordination numbers for Ba. Computational analysis revealed the primarily electrostatic nature of considerably polarised B–N_{amide} and B–$O_{boryloxide}$ bonds. Agostic Ba···H_3C interactions appear instrumental for stabilizing those seemingly coordinatively unsaturated complexes. These compounds are the first molecular catalysts to produce borasiloxanes by dehydrocoupling of borinic acids and hydrosilanes, and we are now working on expanding substrate scope to other such reagents. For instance, the coupling of $PhSiH_3$ with the bulky $\{2,4,6\text{-}^iPr_3\text{-}C_6H_2\}_2BOH$ is mediated by **1** and **2**, albeit the reactions appear to be slower than with R_2BOH (e.g. 37% conversion to $\{2,4,6\text{-}^iPr_3\text{-}C_6H_2\}_2BO\text{-}SiH_2Ph$ is reached after 24 h at 60 °C with [OH]/[SiH]/[Ba] = 10:10:1). On the other hand, with less bulky substrates such as Mes_2BOH, catalysis is for now plagued by the appearance of catalytically inert B–O–B containing species, e.g. $Mes_2B\text{–}O\text{–}BMes_2$ (Mes = mesityl). The catalyzed formation of $\mathbf{P_1}$ is overall kinetically affordable, and we are endeavoring to elucidate the catalytic manifold entwined to the kinetic rate law given by equation (1). In particular, the very negative entropy of activation is compatible with a very organized transition state resulting from nucleophilic attack of the metal-bound oxygen atom onto the incoming silane, much as that seen in the barium-catalyzed dehydrocoupling of amines and hydrosilanes;[32] yet, a simpler σ-bond insertive mechanism cannot be excluded at this stage. All these results will be detailed in a forthcoming report.

Keywords: Barium • boryloxide • low-coordinate complex • dehydrocoupling catalysis • borasiloxane

[1] a) S. Harder, *Chem. Rev.* **2010**, *110*, 3852–3876; b) M. S. Hill, D. J. Liptrot, C. Weetman, *Chem. Soc. Rev.* **2016**, *45*, 972–988.
[2] M. Westerhausen, A. Koch, H. Görls, S. Krieck, *Chem. Eur. J.* **2017**, *23*, 1456–1483.
[3] a) R. Fischer, M. Gärtner, H. Görls, M. Westerhausen, *Angew. Chem. Int. Ed.* **2006**, *45*, 609–612; b) S. Harder, J. Brettar, *Angew. Chem. Int. Ed.* **2006**, *45*, 3474–3478; c) A. S. S. Wilson, M. S. Hill, M. F. Mahon, C. Dinoi, L. Maron, *Science* **2017**, *358*, 1168–1171.
[4] D. Mukherjee, D. Schuhknecht, J. Okuda, *Angew. Chem. Int. Ed.* 10.1002/anie.201801869.
[5] a) B. Maitland, M. Wiesinger, J. Langer, G. Ballmann, J. Pahl, H. Elsen, C. Färber, S. Harder, *Angew. Chem. Int. Ed.* **2017**, *56*, 11880–11884; b) D. Mukherjee, T. Höllerhage, V. Leich, T. P. Spaniol, U. Englert, L. Maron, J. Okuda, *J. Am. Chem. Soc.* **2018**, *140*, 3403–3411.
[6] a) X. Shi, C. Hou, C. Zhou, Y. Song, J. Cheng, *Angew. Chem. Int. Ed.* **2017**, *56*, 16650–16653; b) M. Wiesinger, B. Maitland, C. Färber, G. Ballmann, C. Fischer, H. Elsen, S. Harder, *Angew. Chem. Int. Ed.* **2017**, *56*, 16654–16659.
[7] Y. Sarazin, J.-F. Carpentier, *Chem. Rec.* **2016**, *16*, 2482–2505.
[8] W. D. Buchanan, D. G. Allis, K. Ruhlandt-Senge, *Chem. Commun.* **2010**, *46*, 4449–4465.
[9] K. G. Caulton, M. H. Chisholm, S. R. Drake, K. Folting, *J. Chem. Soc., Chem. Commun.* **1990**, 1349–1351.
[10] O. Poncelet, L. G. Hubert-Pfalzgraf, L. Toupet, J.-C. Daran, *Polyhedron* **1991**, *10*, 2045–2050.
[11] S. R. Drake, W. E. Streib, K. Folting, M. H. Chisholm, K. G. Caulton, *Inorg. Chem.* **1992**, *31*, 3205–3210.
[12] J. Utko, S. Szafert, L. B. Jerzykiewicz, P. Sobota, *Inorg. Chem.* **2005**, 44, 5194–5196.
[13] W. D. Buchanan, M. A. Guino-o, K. Ruhlandt-Senge, *Inorg. Chem.* **2010**, *49*, 7144–7155.
[14] W. A. Wojtczak, M. J. Hampden-Smith, E. N. Duesler, *Inorg. Chem.* **1996**, *35*, 6638–6639.
[15] P. Shao, D. J. Berg, G. W. Bushnell, *Can. J. Chem.* **1995**, *73*, 797–803.
[16] J. A. Darr, S. R. Drake, D. J. Williams, A. M. Z. Slawin, *J. Chem. Soc., Chem. Commun.* **1993**, 866–868.
[17] M. P. Coles, *Coord. Chem. Rev.* **2016**, *323*, 52–59.
[18] S. C. Cole, M. P. Coles, P. B. Hitchcock, *Organometallics* **2004**, *23*, 5159–5168.
[19] R. Pena-Alonso, G. Mariotto, C. Gervais, F. Babonneau, G. D. Soraru, *Chem. Mater.* **2007**, *19*, 5694–5702.
[20] a) W. Liu, M. Pink, D. Lee, *J. Am. Chem. Soc.* **2009**, *131*, 8703–8707.
[21] a) D. A. Foucher, A. J. Lough, I. Manners, *Inorg. Chem.* **1992**, *31*, 3034–3043; b) K. L. Fujdala, A. G. Oliver, F. J. Hollander, T. D. Tilley, *Inorg. Chem.* **2003**, *42*, 1140–1150; c) M. Pascu, A. Ruggi, R. Scopelliti, K. Severin, *Chem. Commun.* **2013**, *49*, 45–47.
[22] a) B. Marciniec, J. Walkowiak, *Chem. Commun.* **2008**, 2695–2697; b) B. Chatterjee, C. Gunanathan, *Chem. Commun.* **2017**, *53*, 2515–2518; c) A. Yoshimura, M. Yoshinaga, H. Yamashita, M. Igarashi, S. Shimada, K. Sato, *Chem. Commun.* **2017**, *53*, 5822–5825.; d) A. Dhakshinamoorthy, A. M. Asiri, P. Concepcion, H. Garcia, *Chem. Commun.* **2017**, *53*, 9998–10001.

[23] M. Ito, M. Itazaki, H. Nakazawa, *J. Am. Chem. Soc.* **2014**, *136*, 6183–6186.

[24] a) B. A. Vaartstra, J. C. Huffman, W. E. Streib, K. G. Caulton, *Inorg. Chem.* **1991**, *30*, 121–125; b) A. G. M. Barrett, M. R. Crimmin, M. S. Hill, G. Kociok-Köhn, D. J. MacDougall, M. F. Mahon, Pa. A. Procopiou, *Organometallics* **2008**, *27*, 3939–3946.

[25] J. S. Alexander, K. Ruhlandt-Senge, *Angew. Chem. Int. Ed.* **2001**, *40*, 2658–2660.

[26] The next closest Ba···H interatomic distance of 3.214(3) Å is too long for a significant interaction.

[27] DFT calculations were performed at the B97-D3/def2-TZVP2 level of theory. See the SI for more details.

[28] Agostic interactions sometimes are rather difficult to pin down unequivocally within the QTAIM framework. See M. Lein, *Coord. Chem. Rev*. **2009**, *253*, 625–634 for further reference. Moreover, the absence of a bonding path does not necessarily prove the non-existence of a stabilising agostic interaction.

[29] The reaction rate for the iminoanilido [{N^N}Ba{N(SiMe$_3$)$_2$.(thf)$_2$] (B. Liu, T. Roisnel, J.-F. Carpentier, Y. Sarazin, *Angew. Chem. Int. Ed.* **2012**, *51*, 4943–4946), 0.62(1) h^{-1}, equalled those for **2** and **2**.(thf)$_2$. Under catalytic conditions, the basic {N^N}$^-$ reacts with R_2BOH to generate a complex akin to **1**, **2**.(thf)$_2$ or **3**. Full release of {N^N}H was detected by NMR upon reaction of [{N^N}Ba{N(SiMe$_3$)$_2$.(thf)$_2$] and 5 equiv of R_2BOH in C_6D_6.

[30] M. S. Hill, D. J. Liptrot, D. J. MacDougall, M. F. Mahon, T. P. Robinson, *Chem. Sci.* **2013**, *4*, 4212–4222.

[31] J. Burés, *Angew. Chem. Int. Ed.* **2016**, *55*, 2028–2031.

[32] C. Bellini, J.-F. Carpentier, S. Tobisch, Y. Sarazin, *Angew. Chem. Int. Ed.* **2015**, *54*, 7679–7683.

Entry for the Table of Contents

COMMUNICATION

The first soluble barium boryloxides have been structurally characterized, and they are shown to act as competent molecular catalysts for the dehydrocoupling of borinic acids with hydrosilanes to generate borasiloxanes under mild conditions.

BORASILOXANE dehydrocoupling catalysis

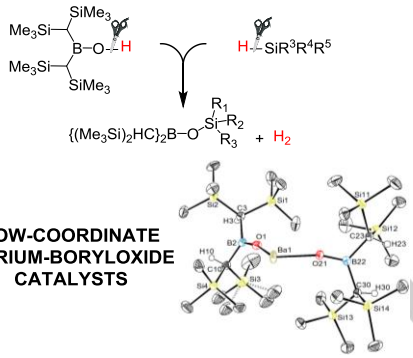

LOW-COORDINATE BARIUM-BORYLOXIDE CATALYSTS

E. Le Coz, V. Dorcet, T. Roisnel, S. Tobisch, J.-F. Carpentier, and Y. Sarazin**

Page No. – Page No.

Low-Coordinate Barium Boryloxides: Synthesis and Dehydrocoupling Catalysis for the Production of Borasiloxanes